doi: 10.21495/71-0-351

25th International Conference
ENGINEERING MECHANICS 2019
Svratka, Czech Republic, 13 – 16 May 2019

FLOW BEHAVIOUR IN COMPRESSION TEST UNDER VARIOUS LUBRICATION CONDITIONS

F. Šebek [*], J. Zapletal [**], P. Kubík [***], J. Petruška [****]

Abstract: *The compression test provides a useful information about the material flow under large plastic deformations, when compared to the standard tensile test. On the other hand, it is heavily dependent on the lubrication conditions. The paper deals with two different specimen geometries resulting in two different friction conditions. The first geometry corresponds to the classical smooth cylinder. The second one was designed according to the idea of Rastegaev. It is a smooth cylinder with grooves on both faces (bases), which allow the lubricant to accumulate and prevent it from escaping the region, where the punches are in the contact with specimen. Then, both cases were computationally simulated and compared with experiments.*

Keywords: Upsetting test, Friction, Equivalent stress, Negative stress triaxiality, Punch.

1. Introduction

The flow curve belongs among the basic inputs into various finite element calculations (Petruška et al., 2016; Peč et al., 2017). It is mostly derived from the standard tensile test and subsequently extrapolated for large plastic deformations (Šebek et al., 2014; Kubík et al., 2017; Šebek et al., 2017a; Španiel et al., 2017). The extrapolation is usually based on a variety of fitting functions for the stress–strain relationship (Jeník et al., 2017). Another possibility of obtaining the flow curve are the punching techniques resulting in equi-biaxial stress state, such as a bulge test (Dick and Yoon, 2018) or small punch test (Šebek et al., 2018). Finally, the flow behaviour can be based on the upsetting test (Hartlen and Doman, 2018). The punching as well as compression testing is complicated by the friction on the contrary to the tensile experiments. The friction has to be dealt with and accounted for in the numerical simulations, but it is difficult to estimate it. Moreover, it violates the equi-biaxial or uniaxial stress state condition. Therefore, there is an effort for eliminating the friction from the process as much as possible. One of the simplest techniques covers the Teflon sheets, which are inserted between the specimen and punches (Xue, 2009). Another approach is based on the modification of the specimen's geometry. Rastegaev (1940) proposed a groove or reservoir at the specimen's faces (bases). This design ensures that the tool (punch) is only in a limited contact with the specimen on its outer diameter and the rest of the contact is transmitted by the fluid (lubricant). It should prevent the specimen from barrelling, which causes the change of the stress state into the triaxial one. Moreover, the specimen is prone to failure earlier in the case of significant barrelling, so larger displacement to failure can be reached by the technique including modified specimen. Accordingly, more reliable data are obtained from the test and extensive extrapolation is not needed.

This paper studies the possibility of developing a Rastegaev-type specimen for a compression and its ability to withstand higher deformations, when compared to a simple smooth cylindrical specimen. Next, a simple technique is presented for a modelling of the liquid as a lubricant without the necessity of using an Euler approach.

[*] Ing. František Šebek, Ph.D.: Institute of Solid Mechanics, Mechatronics and Biomechanics, Faculty of Mechanical Engineering, Brno University of Technology, Technická 2896/2; 616 69, Brno; CZ, sebek@fme.vutbr.cz
[**] Ing. Josef Zapletal, Ph.D.: Institute of Materials Science and Engineering, Faculty of Mechanical Engineering, Brno University of Technology, Technická 2896/2; 616 69, Brno; CZ, zapletal@fme.vutbr.cz
[***] Ing. Petr Kubík, Ph.D.: Institute of Solid Mechanics, Mechatronics and Biomechanics, Faculty of Mechanical Engineering, Brno University of Technology, Technická 2896/2; 616 69, Brno; CZ, kubik.p@fme.vutbr.cz
[****] Prof. Ing. Jindřich Petruška, CSc.: Institute of Solid Mechanics, Mechatronics and Biomechanics, Faculty of Mechanical Engineering, Brno University of Technology, Technická 2896/2; 616 69, Brno; CZ, petruska@fme.vutbr.cz

2. Experiments

The aluminium alloy 2024-T351 was considered. First, the standard tensile tests were carried out in order to obtain the flow curve for simulations. The procedure as well as details and results can be found in Šebek et al. (2017b). It should be noted that the goal was not to obtain the flow curve using the compression experiments. Next, the upsetting tests were conducted. The first ones included the smooth cylindrical specimen (Fig. 1a) and the second ones covered the Rastegaev-type specimens. These were slightly modified, because the marginal edges collapsed during tests (Fig. 1b). Therefore, the final geometry in Fig. 1c was used.

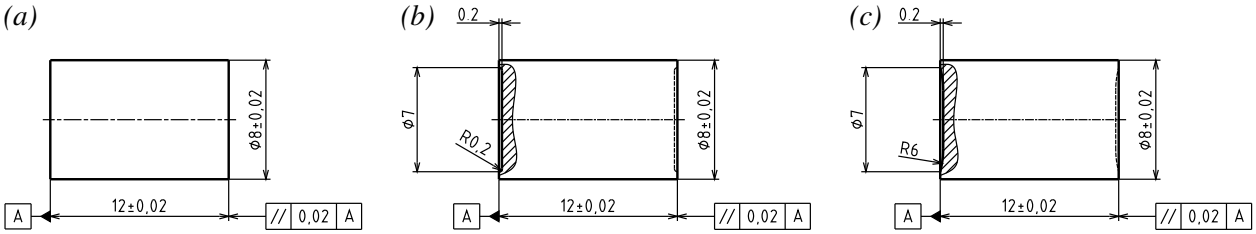

Fig. 1: Detailed drawing of: (a) smooth cylindrical specimen; (b) Rastegaev-type specimen – not used further because of the unwanted edge collapse; (c) Rastegaev-type specimen – used for the further study.

In total, 7 reliable tests were performed, 5 for smooth specimen (Fig. 2a) and 2 for Rastegaev-type one (Fig. 2b). Instron 8801 testing machine with Instron Dynacell ±100 kN dynamic load cell and Instron Clip-On strain gauge extensometer were used. The test speed was 1 mm/min during all experiments under the room temperature. The lubricant OKS 200 MoS_2 (molybdenum disulfide) disposable from −50°C to +450°C was applied.

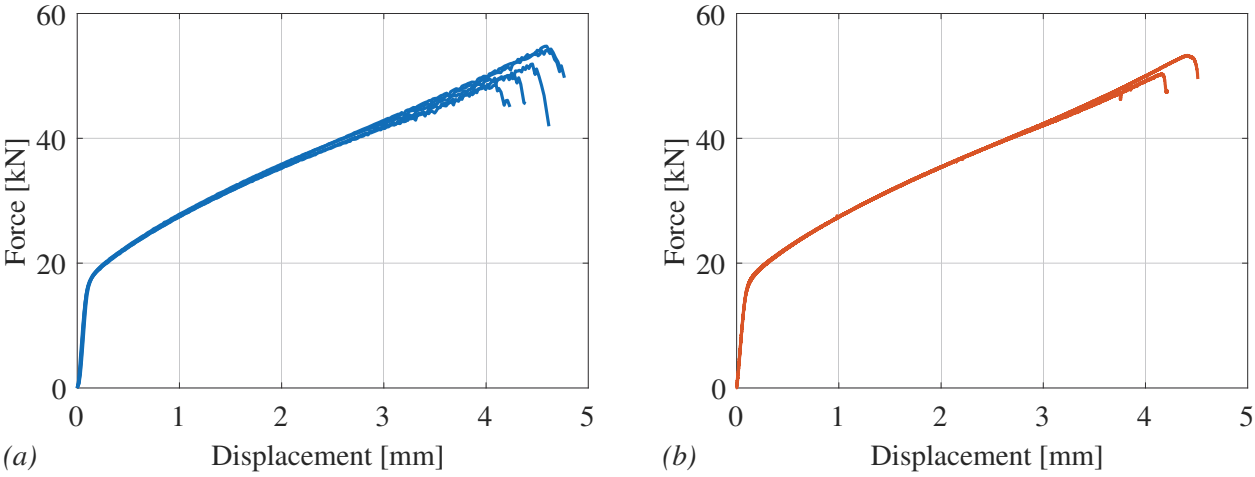

Fig. 2: Compression test results for: (a) smooth specimen; (b) Rastegaev-type specimen.

Post-mortem specimens are shown in Fig. 3. The classical specimens exhibited a slight barrelling, while the Rastegaev-type ones revealed rather anti-barrelling, which approximately formed a hyperboloid-shaped surface.

Fig. 3: Post-mortem: (a) smooth specimens; (b) Rastegaev-type specimens.

3. Simulations

All the simulations were done using Abaqus CAE 2018 without any fracture modelling. The isotropic hardening with associated flow rule was employed according to von Mises. The axial and horizontal symmetries were considered. Punches were meshed with 2-node linear rigid links (RAX2 in Abaqus) and the specimen body by 4-node bilinear quadrilaterals (CAX4R). The characteristic element size was 75 μm. The mesh configurations for specimens are in Fig. 4a and d. The hydraulic definition was determined by the fluid density of 1000 kg·m^{-3} and fluid bulk modulus of 2200 MPa. The auxiliary geometry was needed for defining the fluid cavity as it is required to be a closed area in one part (Fig. 4d). The auxiliary geometry was a very compliant thin strip with Young's modulus of 200 MPa, Poisson's ratio of 0.494 and thickness of 0.1 μm. These characteristics ensure negligible influence on results. The thin strip was in a frictionless contact with punch. The contact between the specimens and punches was modelled with friction coefficient of 0.05.

The field of equivalent plastic strain is plotted on deformed geometries in Fig. 4b and c for both specimens having the same legend. It can be seen that the deformations corresponds to experiments. The deformed shape of Rastegaev-type specimen suggests the reason why the hyperboloid-shaped surface developed – the marginal edge is stiffer and is bended. It is also the reason why the geometry in Fig. 1b collapsed and could not be used due to excessive compliance of the edge.

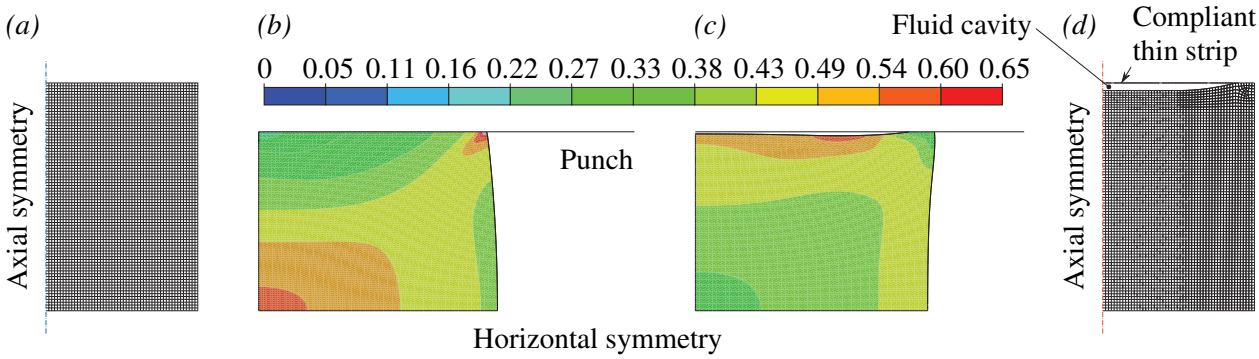

Fig. 4: Numerical simulation: (a) mesh for smooth specimen; (b) equivalent plastic strain for smooth specimen; (c) equivalent plastic strain for Rastegaev-type specimen; (d) mesh for Rastegaev-type specimen.

Fig. 5 shows the force–displacement responses from both the experiments and simulations up to the displacement to fracture. Neither the crack initiation nor its propagation was modelled. All the responses are displayed in one graph so that it is visible that they overlay each other, which proves the correct plasticity model behaviour. The experiments are almost identical for both specimens, while the simulations slightly deviate and exhibit more compliant behaviour (the one of Rastegaev-type with fluid cavity more than the classical one). Nevertheless, the error is negligible in overall.

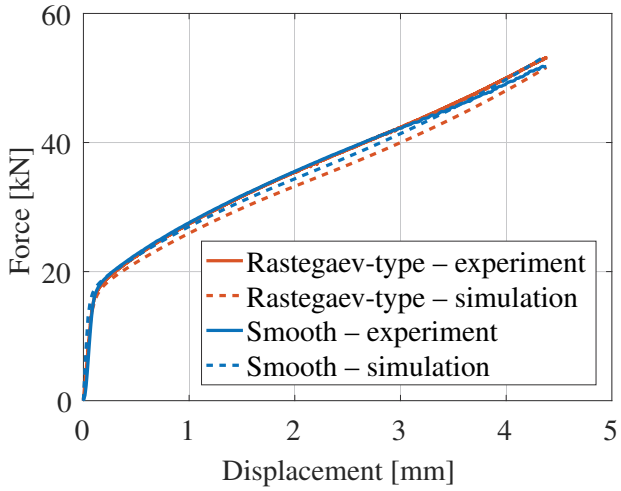

Fig. 5: Force–displacement responses from experiments and simulations.

4. Conclusions

The paper presented a modified geometry of Rastegaev's specimen for upsetting tests. Experiments were conducted on the aluminium alloy 2024-T351, which has a ductility of approximately 20 %. Therefore, it is not very ductile material. Moreover, it does not exhibit significant necking. More ductile materials, such as steels, could show a different behaviour. Especially, the differences between both specimens would be much more distinctive and the displacement to fracture would be prolonged with Rastegaev-type specimen.

Potentially, this could aim to identification of the flow behaviour. Therefore, both situations were modelled with input from standard tensile test in this paper. Both computations exhibited a good agreement with experiments. The advantage of presented modelling is in no need of using a combination of Lagrangian–Eulerian approach (Peč et al., 2016). On the other hand, the presented Rastegaev-type geometry should be redesigned in order to keep it cylindrical as long as possible. Preferably, until fracture in the case of flow curve identification. Nevertheless, there are more similar designs in the literature (Poursina et al., 2008).

Acknowledgments

This work was supported by the Czech Science Foundation under contract No. 19-20802S "A coupled real-time thermo-mechanical solidification model of steel for crack prediction."

References

Dick, R. E. and Yoon, J. W. (2018) Plastic anisotropy and failure in thin metal: Material characterization and fracture prediction with an advanced constitutive model and polar EPS (effective plastic strain) fracture diagram for AA 3014-H19. *International Journal of Solids and Structures*, 151, pp 195–213.

Hartlen, D. C. and Doman, D. A. (2018) A constitutive model fitting methodology for ductile metals using cold upsetting tests and numeric optimization techniques. *Journal of Engineering Materials and Technology*, 141, 1, pp 011008.

Jeník, I., Kubík, P., Šebek, F., Hůlka, J. and Petruška, J. (2017) Sequential simulation and neural network in the stress–strain curve identification over the large strains using tensile test. *Archive of Applied Mechanics*, 87, 6, pp 1077–1093.

Kubík, P., Petruška, J., Hůlka, J. and Šebek, F. (2017) Simulation of the small punch test of AISI 316L austenitic steel. In: *Engineering Mechanics 2017*, Svratka, pp 542–545.

Peč, M., Kubík, P., Šebek, F., Návrat, T. and Petruška, J. (2016) Modeling of the blast load effects in explicit dynamics. In: *Engineering mechanics 2016*, Svratka, pp 442–445.

Peč, M., Vosynek, P., Šebek, F. and Návrat, T. (2017) Implementation of American weld connection standards into finite element computations. In: *IOP Conference Series: Materials Science and Engineering*, 179, pp 012056.

Petruška, J., Návrat, T., Šebek, F. and Benešovský, M. (2016) Optimal intermeshing of multi roller cross roll straightening machine. In: *AIP Conference Proceedings*, 1769, pp 120002.

Poursina, M., Ebrahimi, H. and Parvizian, J. (2008) Flow stress behavior of two stainless steels: An experimental–numerical investigation. *Journal of Materials Processing Technology*, 199, 1–3, pp 287–294.

Rastegaev, M. V. (1940) New method of homogeneous upsetting of specimens for determining the flow stress and the coefficient of internal friction. *Zavodskaja Laboratoria*, pp 354 (in Russian).

Šebek, F., Kubík, P. and Petruška, J. (2014) Localization problem of coupled ductile failure models compared to uncoupled ones. In: *Engineering Mechanics 2014*, Svratka, pp 632–635.

Šebek, F., Petruška, J. and Kubík, P. (2017a) Ductile fracture criteria implementation and calibration using the tension–torsion tests. In: *Engineering Mechanics 2017*, Svratka, pp 854–857.

Šebek, F., Petruška, J. and Kubík, P. (2017b) The performance and prediction ability of advanced approach to ductile fracture. In: *COMPLAS XIV*, Barcelona, pp 588–595.

Šebek, F., Kubík, P. and Petruška, J. (2018) Standard tensile test compared to the small punch test of aluminium alloy. In: *Engineering Mechanics 2018*, Svratka, pp 745–748.

Španiel, M., Mareš, T., Kuželka, J., Šebek, F. and Džugan, J. (2017) Uncoupled material model of ductile fracture with directional plasticity. In: *COMPLAS XIV*, Barcelona, pp 596–605.

Xue, L. (2009) Stress based fracture envelope for damage plastic solids. *Engineering Fracture Mechanics*, 76, 3, pp 419–438.